Hybrid Finite-Horizon Feedback Control for Cart-Pendulum Systems with Uncertainties

Viktor Dodonov*

***Abstract*— A methodology for the design of finite-horizon feedback control strategies is presented, with application to the cart-pendulum system. The control objective is to drive the system from an arbitrary initial state to the desired final state while minimizing the square of the control force. The optimal feedforward control for the linearized model is first derived. It is then converted into a feedback form to improve robustness to uncertainties. To simplify computations during the motion, a linearized feedback controller is introduced. To prevent the increase of the control force near the end of the control interval, an infinite-horizon feedback controller is applied. The effectiveness of the proposed control strategy is demonstrated through numerical experiments in the presence of dynamic and parametric uncertainties. Quasi-optimal trajectories and bounded control effort are achieved, offering a robust and practical solution for finite-horizon control problems.**

I. INTRODUCTION

The problem of designing efficient and reliable control strategies for mechanical systems remains central in control theory and its applications. In many cases, the control objective is to minimize a certain cost functional, such as energy or control effort, over a fixed interval of time. This leads to the class of optimal control problems defined on finite time intervals, known as finite-horizon optimal control [1].

While classical finite-horizon optimal control provides theoretically efficient solutions, it is typically realized in a feedforward (open-loop) form, computed in advance using known system parameters and boundary conditions. However, this strategy often fails in practice due to unavoidable uncertainties in model parameters or unmodeled dynamics. To ensure robustness [2], feedback (closed-loop) control is necessary. It continuously adjusts the control force based on the current state of the system [3]. Yet, practical feedback design methods may not preserve optimality over finite horizons.

This research advances a methodology for constructing finite-horizon feedback control strategies from optimal feedforward solutions. The central idea is to convert a known optimal feedforward control solution into a feedback form that remains optimal (or quasi-optimal) for the nominal system while improving robustness in the presence of uncertainties. This concept was previously demonstrated for simple mechanical systems, such as a point mass and a gravity pendulum, showing that the converted feedback controller can preserve the benefits of the optimal trajectory even under uncertain conditions [4].

*Viktor Dodonov is with LUT School of Engineering Sciences, LUT University, Lappeenranta, Finland viktor.dodonov@lut.fi

In this work, we apply the proposed methodology to a more complex system: the cart-pendulum. This system features both translational and rotational dynamics and is widely used as a benchmark in nonlinear and underactuated control research. The objective is to drive the system from an arbitrary initial state to a desired final state while minimizing the square of the control force:

$$\int_{t_0}^{t_1} u^2\,dt \to \min. \tag{1}$$

A schematic of the cart-pendulum system is shown in Fig. 1. The system dynamics are governed by the following equations:

$$\begin{cases} (M+m)\ddot{X} = u \\ \ddot{x}\cos\varphi + l\ddot{\varphi} + g\sin\varphi = 0 \\ (M+m)(X-x) - ml\sin\varphi = 0 \end{cases} \tag{2}$$

where $x(t)$ is the position of the cart, $\varphi(t)$ is the pendulum angle, $X(t)$ is the horizontal coordinate of the system's center of mass, and $u(t)$ is the control force. The parameters M, m, l, and g denote the mass of the cart, mass of the pendulum, length of the pendulum, and gravitational acceleration, respectively.

Notations. The following symbols will be used throughout the article: the dot $(\dot{q})$ denotes the time derivative, the hat $(\hat{u})$ denotes the optimal feedforward control, the tilde $(\tilde{u})$ denotes the optimal feedback control, and the underline $(\underline{\tilde{u}})$ denotes the linearized form of the optimal feedback control $(\tilde{u})$.

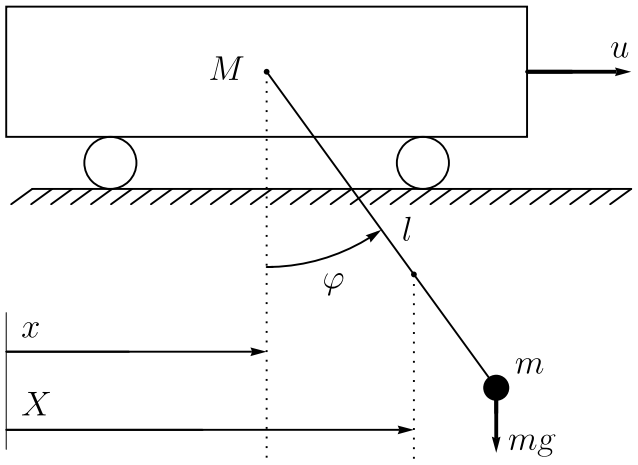

Fig. 1. Schematic of the cart-pendulum system.

II. PROBLEM STATEMENT

We consider the control problem for the cart-pendulum system described by equations (2), where the objective is to drive the system to a desired final state while minimizing the square of the control force. To simplify the analysis and reduce the number of system parameters, we introduce dimensionless variables and parameters.

Let the state variables and control force be scaled as follows:

$$x(t) = l\,\xi(t), \quad X(t) = l\,\eta(t), \quad u(t) = (M+m)\,l\,\upsilon(t), \quad (3)$$

where $\xi(t)$ and $\eta(t)$ are the dimensionless positions of the cart and the center of mass, respectively, and $\upsilon(t)$ is the dimensionless control force.

We also introduce the dimensionless parameter μ and define ω, Ω so that

$$\mu = \frac{M}{M+m}, \qquad \omega^2 = \frac{g}{l}, \qquad \Omega^2 = \frac{\omega^2}{\mu}, \quad (4)$$

where Ω (with units of $1/\mathrm{s}$) is chosen such that it appears as the natural frequency in the expression for the optimal control force in the linearized system. This simplifies the structure of the resulting control law.

In the new variables, the nonlinear equations of motion (2) take the form:

$$\begin{cases} \ddot{\eta} = \upsilon \\ \ddot{\xi}\cos\varphi + \ddot{\varphi} + \mu\,\Omega^2 \sin\varphi = 0 \\ \eta - \xi - (1-\mu)\sin\varphi = 0 \end{cases} \quad (5)$$

To design the optimal control, we linearize the system around the upright position $\varphi = 0$. The resulting linearized model is:

$$\begin{cases} \ddot{\eta} = \upsilon \\ \ddot{\eta} + \mu\,\ddot{\varphi} + \mu\,\Omega^2\varphi = 0 \end{cases} \quad (6)$$

The performance criterion is the same as introduced in (1), now written in terms of the dimensionless control force:

$$(M+m)^2\,l^2 \int_{t_0}^{t_1} \upsilon^2\,dt \to \min. \quad (7)$$

The goal of the study is to design a feedback control $\upsilon(t)$ that minimizes the functional (7) for the linearized model (6), and then to analyze its performance when applied to the full nonlinear system (5), especially in the presence of parametric uncertainties.

III. METHODOLOGY

To derive the optimal control strategy for the linearized model (6) with the cost functional (7), we consider the augmented functional

$$\int_{t_0}^{t_1} \ddot{\eta}^2 + \lambda(\ddot{\eta} + \mu\,\ddot{\varphi} + \mu\,\Omega^2\varphi)\,dt \to \min. \quad (8)$$

where $\lambda(t)$ is a Lagrange multiplier enforcing the second equation in (6) as a constraint. The functional (8) represents the squared control force $\ddot{\eta} = \upsilon$ subject to the dynamic constraint that couples η and φ.

Applying the Euler-Lagrange equation to this constrained problem leads to the following necessary conditions for optimality [5]:

$$\begin{cases} \ddot{\lambda} + \Omega^2\lambda = 0 \\ \ddot{\upsilon} + \ddot{\lambda} = 0 \\ \ddot{\eta} - \upsilon = 0 \\ \ddot{\eta} + \mu\,\ddot{\varphi} + \mu\,\Omega^2\varphi = 0 \end{cases} \quad (9)$$

The first equation is a harmonic oscillator equation for λ, while the remaining equations describe the coupling between υ, η, and φ. The resulting system forms a boundary value problem in time, with conditions specified at both the initial time t_0 and the final time t_1.

The general solution for the optimal control force $\upsilon(t)$ has the form

$$\upsilon(t) = c_0 + c_1 t + c_2\sin(\Omega t) + c_3\cos(\Omega t), \quad (10)$$

where c_0, c_1, c_2, c_3 are constants.

Substituting the optimal control expression (10) into the necessary conditions (9), we arrive at the following system:

$$\begin{cases} \ddot{\eta} = c_0 + c_1 t + c_2\sin(\Omega t) + c_3\cos(\Omega t) \\ \mu\,\ddot{\varphi} + \mu\,\Omega^2\varphi = -c_0 - c_1 t - c_2\sin(\Omega t) - c_3\cos(\Omega t) \end{cases} \quad (11)$$

The constants c_0, c_1, c_2, c_3 are determined by applying the boundary conditions, which specify the system's state at the initial t_0 and final t_1 times.

The control interval is re-centered for convenience, using

$$t_0 = -T, \qquad t_1 = 0, \quad (12)$$

so that the motion ends at time $t = 0$.

The boundary conditions for the optimization problem are chosen as

$$\begin{cases} \eta(-T) = \eta_0 \\ \dot{\eta}(-T) = \dot{\eta}_0 \\ \varphi(-T) = \varphi_0 \\ \dot{\varphi}(-T) = \dot{\varphi}_0 \end{cases} \qquad \begin{cases} \eta(0) = 0 \\ \dot{\eta}(0) = 0 \\ \varphi(0) = 0 \\ \dot{\varphi}(0) = 0 \end{cases} \quad (13)$$

which correspond to arbitrary initial conditions and zero final state, as in a typical stabilization task.

Solving the system (11) under the boundary conditions (13) allows one to determine the coefficients c_0, c_1, c_2, c_3 as functions of the initial state and the control duration T. The resulting expression for $\hat{\upsilon}(t)$ represents the optimal non-feedback control. The explicit expressions are algebraically involved and omitted here for brevity.

To convert the resulting optimal control $\hat{\upsilon}$ into feedback form $\tilde{\upsilon}$, we follow the substitution strategy proposed in [4]. Since the optimal control was derived over the interval $[-T, 0]$, we substitute the current time t as the initial time $-T$. The total control duration T is replaced by the remaining time $T - t$, capturing the idea that the system is always starting from its current state and time, with a reduced time horizon. At the same time, the initial conditions η_0, $\dot{\eta}_0$, φ_0, $\dot{\varphi}_0$ are replaced by the current values $\eta(t)$, $\dot{\eta}(t)$, $\varphi(t)$, $\dot{\varphi}(t)$, thus turning the open-loop control into a time-varying

feedback controller that adapts in real time. The time variable t in the control expression is kept as is, reflecting the ongoing evolution within the remaining control interval.

$$\begin{aligned} t &\to -T, & \eta_0 &\to \eta(t), & \varphi_0 &\to \varphi(t), \\ T &\to T-t, & \dot\eta_0 &\to \dot\eta(t), & \dot\varphi_0 &\to \dot\varphi(t). \end{aligned} \tag{14}$$

The resulting expression defines the optimal feedback control $\tilde\upsilon(t)$, which preserves the structure of the optimal control in the nominal system while introducing robustness to uncertainties and disturbances.

When the remaining control time is not large, the system approaches the equilibrium, and the nonlinear effects become less significant. In this regime, the linearized form of the feedback controller can be used as commonly done for near-equilibrium control design [6]. The control law is given by

$$\begin{aligned} \underline{\tilde\upsilon} = &-\left(\frac{840\mu}{\tau^4\omega^2} - \frac{20}{3\tau^2} + \frac{7\omega^2}{594\mu}\right)\eta(t) \\ &-\left(\frac{480\mu}{\tau^3\omega^2} - \frac{88}{21\tau} + \frac{160\tau\omega^2}{14553\mu}\right)\eta'(t) \\ &-\left(\frac{840\mu^2}{\tau^4\omega^2} - \frac{380\mu}{3\tau^2} + \frac{8761\omega^2}{4158}\right)\varphi(t) \\ &-\left(\frac{480\mu^2}{\tau^3\omega^2} - \frac{424\mu}{21\tau} + \frac{2008\tau\omega^2}{14553}\right)\varphi'(t), \end{aligned} \tag{15}$$

where $\tau = T - t$ denotes the remaining control time. In the numerical experiments, this linearized feedback control is applied during the second half of the motion interval to simplify implementation while preserving quasi-optimality near the equilibrium.

IV. NUMERICAL RESULTS

To evaluate the performance of the proposed feedback control strategy, we apply it to the cart-pendulum system using the following parameters and initial conditions:

$$\begin{aligned} M &= 2.5\ \text{kg}, & \mu &= 0.25, & x_0 &= -20\ \text{m}, \\ m &= 7.5\ \text{kg}, & \omega &= 0.7\ \text{s}^{-1}, & \dot x_0 &= 0\ \text{m s}^{-1}, \\ l &= 20\ \text{m}, & \Omega &= 1.4\ \text{s}^{-1}, & \varphi_0 &= 0\ \text{rad}, \\ g &= 9.8\ \text{m s}^{-2}, & T &= 10\ \text{s}, & \dot\varphi_0 &= 0\ \text{rad s}^{-1}. \end{aligned} \tag{16}$$

These values correspond to a relatively heavy pendulum mounted on a light cart, with the goal of bringing the system to the origin from a distant initial position. The initial pendulum angle is zero.

Fig. 2 shows the behavior of the linear (6) and nonlinear (5) systems under feedforward $\hat\upsilon$ and feedback $\tilde\upsilon$ control strategies, both derived from the linear model. The feedback control strategy includes a switch at $t = T/2$ from the nonlinear form $\tilde\upsilon$ to its linearized form $\underline{\tilde\upsilon}$.

The top plot of Fig. 2, corresponding to the center of mass η, shows that all controllers lead the center of mass $\eta(t)$ to the required final position along the same trajectory, except for the feedback control applied to the nonlinear system, which also reaches the target but shows slight deviations during the final second of motion.

The middle plot of Fig. 2, corresponding to the pendulum angle φ, shows small differences between the trajectories,

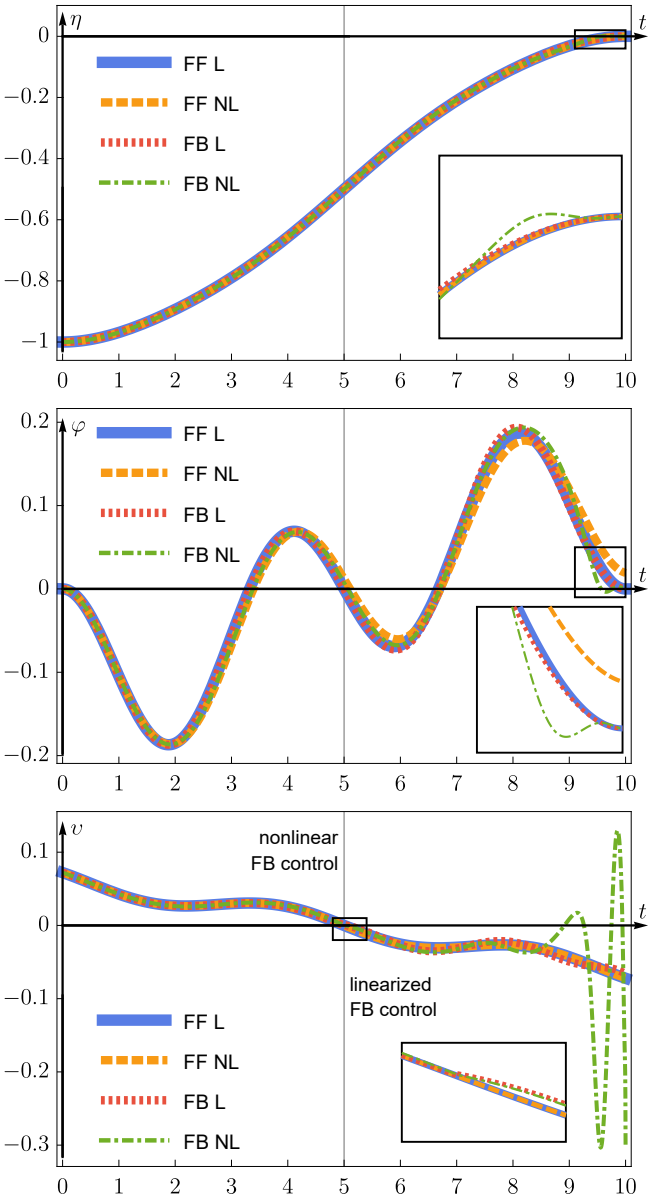

Fig. 2. System response under feedforward (FF) and feedback (FB) control strategies derived from the linearized model and applied to either the linear (L) or nonlinear (NL) system. The vertical line at $t = T/2$ indicates the moment when the feedback control switches from nonlinear to linearized form. From top to bottom, the plots show the evolution of the center of mass $\eta(t)$, pendulum angle $\varphi(t)$, and control force $\upsilon(t)$.

especially near the end of the motion. While both feedforward and feedback control strategies perform well on the linear system, the feedforward control fails to stabilize the pendulum in the nonlinear case. The feedback controller, on the other hand, succeeds in bringing the pendulum close to zero, though there is a small deviation during the final second of motion.

The bottom plot of Fig. 2, corresponding to the control force υ, shows a slight deviation in the feedback trajectories beginning at $t = T/2$, where the controller switches from nonlinear to linearized form. In the nonlinear system, the feedback controller shows an increase in control effort with

small oscillations toward the end of the motion. This is due to the controller actively compensating for dynamic uncertainty. As shown in the top plot, despite these fluctuations, the system still reaches the required final position.

Before moving on to experiments with parametric uncertainties, we introduce a softer control strategy to avoid the increase in control force near the end of the motion. As seen in the linearized feedback control law (15), the coefficients tend to infinity as the remaining control time τ approaches zero. To address this, we introduce an infinite-horizon optimal controller [7] that minimizes the cost functional

$$\int_0^\infty \eta^2 + \varphi^2 + 0.01\dot{\eta}^2 + 0.01\dot{\varphi}^2 + \upsilon^2\, dt \to \min. \qquad (17)$$

This controller is activated at the final stage of motion in the next set of experiments, where the presence of parametric uncertainties makes robustness and stability even more critical.

Fig. 3 shows the behavior of the nonlinear system under feedforward control strategy $\hat{\upsilon}$ derived from the nonlinear model, and feedback control strategy $\tilde{\upsilon}$ derived from the linear model. The feedback control strategy includes a switch at $t = 5\,\mathrm{s}$ from the nonlinear form $\tilde{\upsilon}$ to its linearized form $\underline{\tilde{\upsilon}}$, followed by a second switch at $t = 8.5\,\mathrm{s}$ to the infinite-horizon feedback controller.

The top plot of Fig. 3, corresponding to the center of mass η, shows that all controllers guide the system along nearly identical trajectories, even in the presence of both parametric and dynamic uncertainties. The infinite-horizon controller can be tuned to limit the maximum deviation near the end of the motion, making it a flexible final-stage strategy.

The middle plot of Fig. 3, corresponding to the pendulum angle φ, shows small differences between the trajectories, though all remain smooth and close to the nominal path under feedback control, even with uncertainties present.

The bottom plot of Fig. 3, corresponding to the control force υ, shows a slight deviation in the feedback controllers prior to the switch to the infinite-horizon strategy. The transition at $t = 8.5\,\mathrm{s}$ causes a sharp change in control force, although the state variables remain smooth. In practice, smooth transitions between controllers can be achieved using practical techniques for bumpless transfer [8], [9].

The numerical results confirm the effectiveness of the proposed feedback control strategy in guiding the cart-pendulum system to the desired final state, even in the presence of dynamic and parametric uncertainties. The use of a switching mechanism between finite-horizon nonlinear feedback, finite-horizon linearized feedback, and infinite-horizon feedback controllers enables quasi-optimal motion and bounded control during implementation.

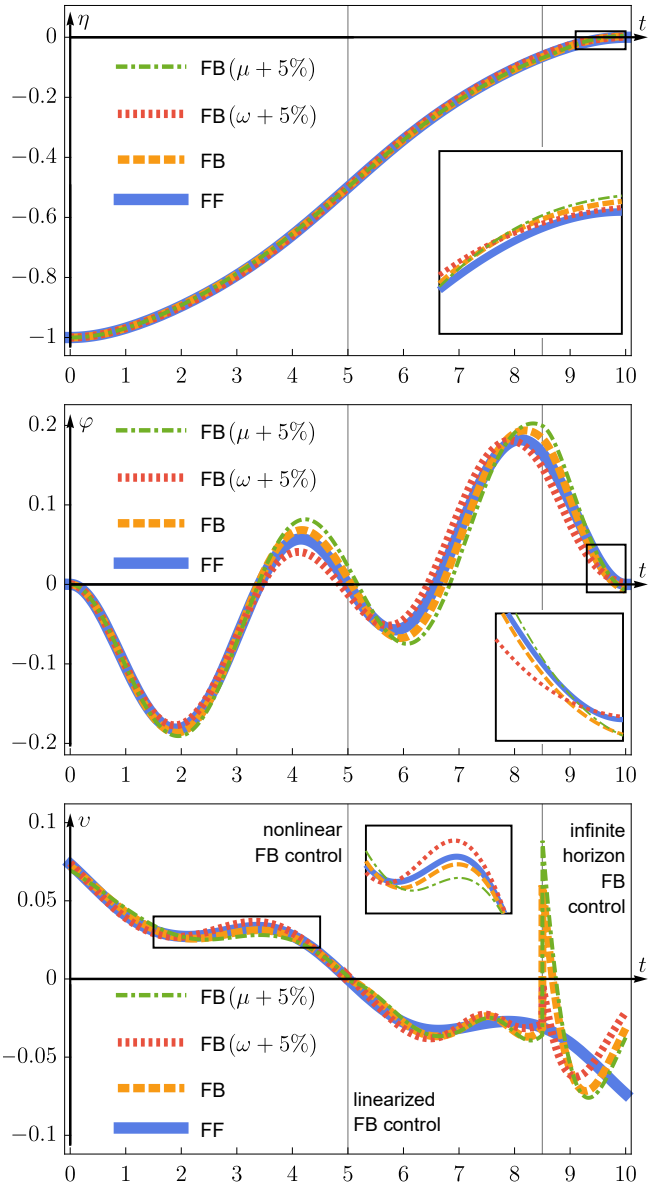

Fig. 3. System response under feedforward (FF) control strategy derived from the nonlinear model, and feedback (FB) control strategies derived from the linear model, all applied to the nonlinear system. Labels $(\omega+5\%)$ and $(\mu+5\%)$ indicate feedback controllers designed using perturbed system parameters. The vertical line at $t = 5\,\mathrm{s}$ marks the switch from nonlinear to linearized feedback control. The second vertical line at $t = 8.5\,\mathrm{s}$ marks the transition from linearized feedback to an infinite-horizon feedback controller. From top to bottom, the plots show the evolution of the center of mass $\eta(t)$, pendulum angle $\varphi(t)$, and control force $\upsilon(t)$.

V. CONCLUSION

This work presents a methodology for designing finite-horizon feedback control strategies for mechanical systems, illustrated by the cart-pendulum example. The approach is based on converting the optimal feedforward control, derived for the linearized system, into a real-time feedback control law. To simplify computations during the second half of the motion, a linearized form of the feedback control is used. At the final stage, an infinite-horizon feedback controller is introduced to handle the increase of the control effort as the remaining time approaches zero.

The performance of the proposed strategy is evaluated through numerical experiments, demonstrating successful stabilization of both linear and nonlinear models, even in the presence of uncertainties. The feedback control maintains quasi-optimal trajectories while compensating for model

imperfections and uncertainties. The use of infinite-horizon control at the final stage provides a smooth and bounded control action near the equilibrium.

The results indicate that the proposed methodology offers a flexible and robust solution for finite-horizon optimal control problems, particularly in systems subject to nonlinearities and parameter variations. Future work will focus on experimental validation of the control strategy, for example, through its implementation on a levitating linear motion platform. The model of this system is presented in [10], and the control concept discussed in this paper shows good preliminary simulation results using that model. However, physical experiments have not yet been performed. The development of smooth transition strategies between different controllers in physical setups is also identified as an important direction for future research.

REFERENCES

[1] L. T. Ashchepkov, D. V. Dolgy, T. Kim, and R. P. Agarwal, *Optimal Control*. Cham: Springer, 2021.

[2] K. Zhou and J. C. Doyle, *Essentials of Robust Control*. New Jersey: Prentice Hall, 1998.

[3] E. F. Camacho and C. Bordons, *Model Predictive Control*. London: Springer, 2007.

[4] V. Dodonov, "Finite-horizon optimal feedback control design illustrated by point mass and gravity pendulum cases," in *10th International Conference on Control, Decision and Information Technologies (CoDIT)*, 2024, pp. 1798–1803.

[5] F. Rindler, *Calculus of Variations*. Cham: Springer, 2018.

[6] H. K. Khalil, *Nonlinear Systems*, 3rd ed. New Jersey: Prentice Hall, 2002.

[7] B. D. O. Anderson and J. B. Moore, *Optimal Control: Linear Quadratic Methods*. New Jersey: Prentice Hall, 1990.

[8] S. Skogestad and I. Postlethwaite, *Multivariable Feedback Control: Analysis and Design*, 2nd ed. Wiley, 2005.

[9] A. Smirnov, K. Tolsa, and R. P. Jastrzebski, "Implementation of a bumpless switch in axial magnetic bearings," in *International Symposium on Industrial Embedded System (SIES)*, 2010, pp. 63–68.

[10] A. Putkonen, S. Madanzadeh, V. Dodonov, A. Zhuravlev, L. Chechurin, and R. P. Jastrzebski, "Modeling and control of a levitating linear motion platform," in *2024 International Conference on Electrical Machines (ICEM)*, 2024, pp. 1–8.